PROBING THE NON-LINEAR DYNAMICS OF THE ESRF STORAGE RING WITH EXPERIMENTAL FREQUENCY MAPS

Y. Papaphilippou, L. Farvacque, A. Ropert, ESRF, Grenoble, France
J. Laskar, ASD-IMCEE, Paris, France

Abstract

A key issue for improving the performance of third generation light sources like the ESRF storage ring is the identification and correction of resonances that have a detrimental effect in the machine performance. Frequency analysis of experimental data, recorded on BPMs around the ring, is a powerful tool for studying the non-linear dynamics of an accelerator in operation. In a series of experiments, experimental frequency maps were produced using the 1000-turns measurement system. These maps revealed the resonance structure in the vicinity of the nominal working point which was limiting the dynamic aperture. Their comparison with maps produced by simulations was used as a guide for understanding the storage ring non-linear model. The possibility of using the quasi-periodic approximations of the experimental data for testing the efficiency of resonance correction schemes was finally investigated.

INTRODUCTION

The beam lifetime, determined by the electron beam loss rate, is one of the key parameters for evaluating the performance of a synchrotron light source. It depends strongly on collision mechanisms with other electrons or residual gas, effects which are associated with the collective behaviour of the beam and its interaction with the environment (e.g. the vacuum quality). On the other hand, single particle motion, dominated by the applied non-linear magnetic fields, can become chaotic and particles may diffuse to large amplitudes through non-linear resonances, enhancing the particle loss. It is the interplay of these two mechanisms that reduces the beam lifetime [1]. In recent years, methods coming principally from celestial mechanics [2], such as the frequency map analysis (FMA), have been successfully used in order to study the single particle non-linear dynamics in accelerators. Apart from the already established power of the methods when applied in simulations in order to display and understand the global beam dynamics [3], they have been very successfully applied for analysing experimental data of excited transverse beam oscillations, recorded turn by turn on beam position monitors [1, 4, 5]. In this paper, we will present the first feasibility test made at the ESRF storage ring, in order to produce experimental frequency maps, by using the 1000-turn measurement system [6]. These tests are the first step towards studying and understanding the limitations of the horizontal dynamic aperture observed at the storage ring in various experimental machine studies [7].

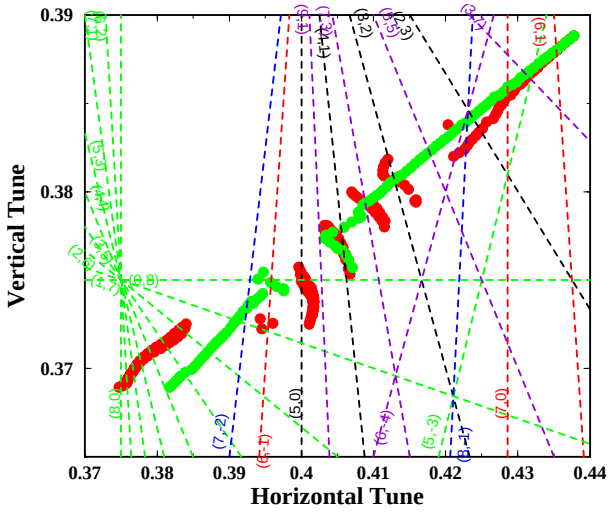

Figure 1: Experimental frequency map of the ESRF ring. The red curve corresponds to the frequencies computed by an analysis of all 252 turns, whereas the green curve corresponds to the frequencies computed for a time-span equal to the decoherence time.

FREQUENCY MAP ANALYSIS

In brief, the FMA enables the derivation of a quasi-periodic approximation $f'(t) = \sum_{k=1}^{N} a_k e^{i2\pi\nu_k t}$, truncated to order N, of a complex function $f(t) = q(t)+ip(t)$, formed by a pair of conjugate variables, which are determined numerically or experimentally. The frequency ν_1 of the first term is associated with the fundamental frequency of motion. Applying the method to a large number of orbits with different initial conditions enables the creation of a very detailed tune footprint, the frequency map. Due to the very high precision of the tune determination through a refined Fourier analysis using the NAFF algorithm [2], all the excited resonances appear as line distortions of this map. The application of the method to experimental data can reveal the complex network of resonances associated with non-linear motion in a real accelerator [4]. A second aspect of the method, is the study of the quasi-periodic approximation itself for each excited orbit [5]. All terms of this approximation are decomposed as a linear combination of the fundamental frequencies $\nu_k = k_x\nu_x + k_y\nu_y$. The amplitudes $a_k \equiv a_{(k_x,k_y)}$ of these terms are associated with the driving terms of a resonance $m_x\nu_x + m_y\nu_y = c$ with: a) $(m_x, m_y) = (-k_x + 1, -k_y)$ for horizontal and b) $(m_x, m_y x) = (-k_x, -k_y + 1)$ for vertical motion. Thereby, the excitation of an individual resonance can be determined by computing or measuring these amplitudes.

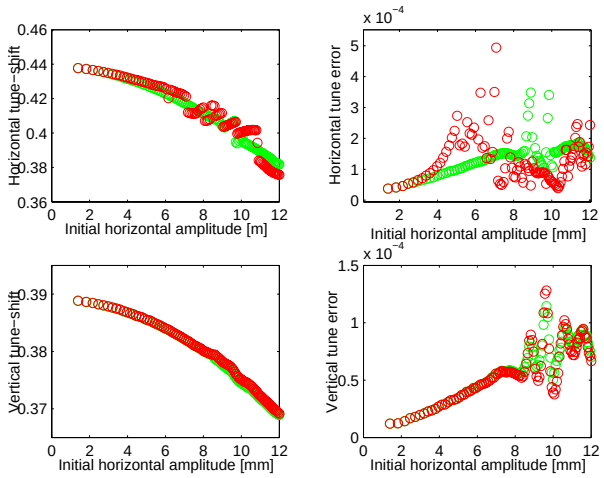

Figure 2: Horizontal [top] and vertical [bottom] tune-shift [right] and tune-error [left] with amplitude. The colour-code of the two curves is the same as in Fig. 1.

EXPERIMENTAL FREQUENCY MAPS

In a series of experiments, we have performed several tests for setting up and automating the procedure for the production of experimental frequency maps. We used an electron bunch train of around 5mA total current, filing 1/3 of the machine circumference. The machine tunes were set to the nominal ones $(36.44, 14.39)$ and the chromaticity was set to zero in order to limit the beam decoherence time. The beam was excited synchronously with one of the four horizontal fast injection kickers and a vertical shaker. The kicker and shaker currents were automatically controlled and 104 horizontal times 3 vertical kicks were applied, giving a total of 312 orbits. The whole experiment lasted about 4 hours. The maximum horizontal kicker current was set to a value where beam losses start to occur. This corresponds to an horizontal displacement of 12 mm in the middle of the straight section where $\beta_x = 35.1$ m. The shaker was limited by technical problems giving a maximum vertical displacement of 0.8 mm in the middle of the straight section, where $\beta_y = 2.5$ m (40% of the vertical physical aperture).

The data was recorded on the 214 BPMs of the storage ring for 256 turns and post-processed with a MatLab [8] version of the frequency analysis algorithm. The tunes were extracted on each BPM and the results of the average tune from all the BPMs for each measurement are plotted in the frequency map of Fig. 1. The red curve corresponds to the tunes obtained by an application of the frequency analysis algorithm to the full length of data (252 turns). However, for high amplitudes, due to the amplitude dependent tune-shift, the beam decoheres very rapidly leaving a few tens of turns available to be analysed. The green curve corresponds to the analysis of the data of the oscillations that are still coherent. The two curves are roughly the same apart from the obvious deviation at large amplitude and the fact that the second one is more linear and less distorted. Due to the fact that the vertical amplitudes are very small, the tune-shift in both directions is mostly due to the horizontal excursion of the beam, as can be seen in Fig. 2, where the horizontal and vertical tune-shift is plotted as a function of the horizontal initial amplitude in the middle of the straight section. In the same figure, the statistical error in the tune determination is also displayed, defined through the standard deviation over the measured tune values on all the BPMs. As this error is a measure of the tune precision, it depends on the length of the analysed data but also on the regularity of the phase space for each measured orbit. Indeed, the tune error is less then 10^{-4} for most cases, whereas in the vicinity of a resonance it gets higher. Finally, note that the statistical error in the determination of the horizontal tune is higher than the one of the vertical tune, as the beam excursion and thus the influence of non-linear fields is stronger in the horizontal plane.

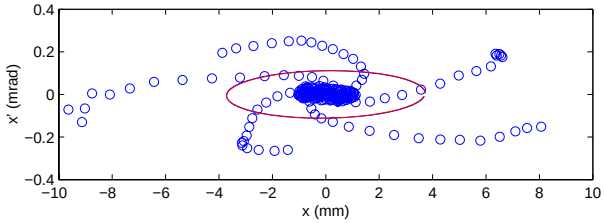

Figure 3: Horizontal phase space plot in the vicinity of the (5,0) resonance.

The map can be roughly separated in three regions: For small amplitudes and up to 7 mm amplitude, the detuning with amplitude seems to have a regular behaviour. Between 7 and 11 mm amplitudes, there is a zone of instability characterised by the accumulation of points on resonant lines or gaps. Most of the resonances are of the fifth or tenth order: (5,0), (4,1), (3,2), (9,1), (7,3), (6,4) and (5,5). A projection of the phase space motion on the horizontal plane, in the vicinity of the (5,0) resonance, is presented in Fig. 3. The resonant behaviour of motion is obvious. Finally, for bigger amplitudes (from 11 up to 12 mm amplitude), the tune path is regular, crossing a multitude of 8th order resonances that are not excited. The last point, where losses begin to occur, approaches an area of potential instability, the crossing point of all third order resonances and the coupling resonances $(1, -1)$. A frequency map resulting from a numerical simulation of a model, with measured focusing and coupling errors included and corrected, is presented in Fig. 4. These first numerical results suggest that the excited zone in the vicinity of the 3rd order resonance is large enough to induce beam loss as far as the last measured tunes in this experiment.

RESONANCE DRIVING TERMS

In Fig. 5, the strength of the fifth order resonance $(5, 0)$ driving term is plotted, for initial conditions in its vicinity, as measured by the corresponding $a_{(-4,0)}$ amplitude of the quasi-periodic approximation. In the top plot, the driving term mean values over the measurements given by all the BPMs with error-bars representing their standard deviation are plotted versus the initial horizontal amplitudes of the kicked beam. The resonance driving term is increasing

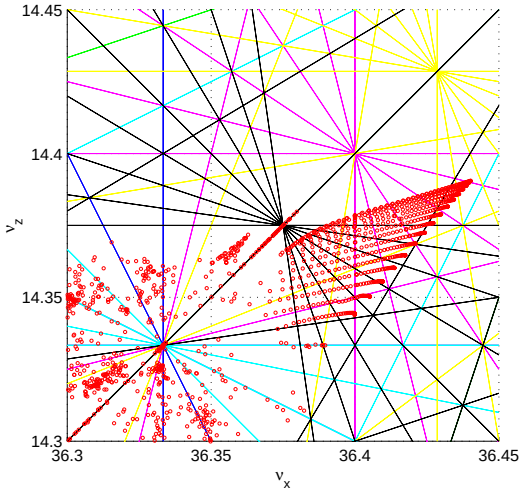

Figure 4: Frequency map for the ESRF model.

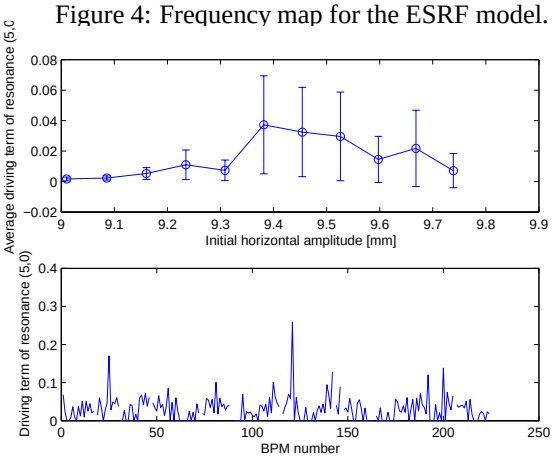

Figure 5: Average (5,0) resonance driving term and its variation along the ring for one particular beam excitation.

as the particles approach the resonance and then decreases gradually to very small values after the resonance has been crossed. In the bottom plot, the behaviour of the resonance driving term along the ring is displayed. The maximum values of the driving term are reached in areas where the horizontal beta function takes large values (higher than 25 m).

Another driving term associated with to the horizontal 3rd integer resonance is plotted in Fig. 6. In order to increase the measurement's sensitivity, the lattice was matched to a working point close to this resonance and 4 small kicks of increasing horizontal amplitude were applied. The two curves correspond to measurements before and after switching on the sextupole corrector and, indeed, the resonance driving term drops, after the correction.

CONCLUSIONS AND PERSPECTIVES

We presented the first results from the application of the frequency map analysis technique to experimental beam data of the ESRF storage ring. This was mostly a feasibility study for testing the efficiency of the method with respect to the available hardware and diagnostics. The preliminary results revealed many unknown features of the electron dynamics for the nominal working point of the ESRF storage ring. Moreover, it was confirmed that the limitation of the

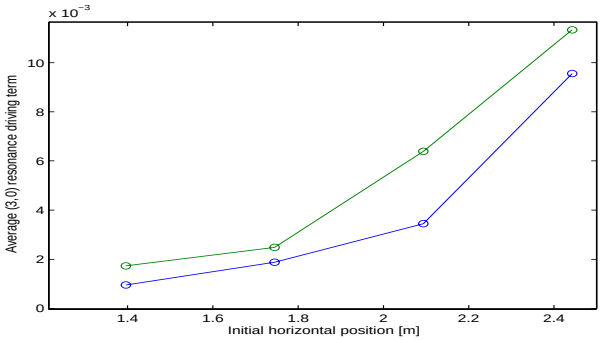

Figure 6: Comparison between the normal sextupole (3,0) resonance driving term along the ring with (green) and without (blue) sextupole correction.

horizontal dynamic aperture is due to an interplay between third order resonances. At the same time, a variety of questions were raised with respect to the reason for this resonance excitation. A detailed non-linear dynamics' analysis assisted by particle tracking is underway in order to refine the non-linear model. One of the practical limitations of the method is the long acquisition time [6]. A dedicated "frequency map" BPM has been tested and the first results were very promising [9]. The development of this system in addition with the installation of a strong vertical kicker will enable the construction of a frequency map for beam amplitudes up to the full ring aperture in a few minutes. Finally, the problem of beam decoherence and the ambiguity it introduces in the tune determination is been currently under careful study. One of the perspectives is establishing a method for a very accurate tune determination using the information from all the BPMs, for a few turns.

We would like to thank P. Elleaume, E. Plouviez, J.-L. Revol, K. Scheidt and the ESRF operation group for their help in the course of these experiments.

REFERENCES

[1] C. Steier, et al., PRE 65, 056506, 2002; Nadolski et al., submitted to PRST-AB.

[2] J. Laskar, Astron. Astroph. 198, 341, 1988; Icarus 88, 266, 1990; Physica D 67, 257 1993; NATO-ASI, S'Agaro, Spain, 1996; J. Laskar, et al., Physica D 56, 253, 1992; Y. Papaphilippou et al., Astron. Astroph. 307, 427 , 1996; Astron. Astroph. 329, 451, 1998.

[3] H.S. Dumas et al., Phys. Rev. Let. 70, 2975, 1993; J. Laskar et al., Part. Accel. 54, 183, 1996; Y. Papaphilippou, PAC'99, New York, 1999; PAC'01, Chicago, 2001; Y. Papaphilippou et al., PRST-AB 2, 104001,1999; PRST-AB 5, 074001, 2002;

[4] D. Robin et al., Phys. Rev. Let. 85, 558, 2000; L. Nadolski, PhD thesis, CEA, 2001; A.L. Robinson, CERN Courier, Vol 41, N.1, 2001.

[5] R. Bartolini et al., PAC'99, New York, 1999; Schmidt et al., PAC'01, 2001; Hayes et al, EPAC'02, 2002; R.Tomas, PhD Thesis, CERN 2003.

[6] L. Farvaque et al., DIPAC 2001, Grenoble, 2001.

[7] A. Ropert, ESRF notes 13-98/MDT, 20-98/MDT, 12-01/MDT, 1301/MDT, 12-02/MDT.

[8] MatLab, The MathWorks, Natick, MA

[9] E. Plouviez, private communication.